Jastrow-type calculations of one-nucleon removal reactions on open *s-d* shell nuclei

M. K. Gaidarov, K. A. Pavlova, and A. N. Antonov
Institute of Nuclear Research and Nuclear Energy, Bulgarian Academy of Sciences, Sofia 1784, Bulgaria

C. Giusti
Dipartimento di Fisica Nucleare e Teorica, Università di Pavia, Istituto Nazionale di Fisica Nucleare, Sezione di Pavia, Pavia, Italy

S. E. Massen and Ch. C. Moustakidis
Department of Theoretical Physics, Aristotle University of Thessaloniki, GR-54006 Thessaloniki, Greece

K. Spasova
Department of Theoretical and Applied Physics, "Bishop K. Preslavski" University, Shumen 9712, Bulgaria
(Received 11 October 2001; revised manuscript received 17 October 2002; published 5 December 2002)

Single-particle overlap functions and spectroscopic factors are calculated on the basis of Jastrow-type one-body density matrices of open-shell nuclei constructed by using a factor cluster expansion. The calculations use the relationship between the overlap functions corresponding to bound states of the $(A-1)$-particle system and the one-body density matrix for the ground state of the A-particle system. In this work, we extend our previous analyses of reactions on closed-shell nuclei by using the resulting overlap functions for the description of the cross sections of (p,d) reactions on the open s-d shell nuclei ^{24}Mg, ^{28}Si, and ^{32}S and of ^{32}S$(e,e'p)$ reaction. The relative role of both shell structure and short-range correlations incorporated in the correlation approach on the spectroscopic factors and the reaction cross sections is pointed out.

DOI: 10.1103/PhysRevC.66.064308 PACS number(s): 21.60.−n, 21.10.Jx, 25.40.Hs, 25.30.Dh

I. INTRODUCTION

Nowadays consistent efforts in the correct treatment of the beyond mean-field nucleon-nucleon (*NN*) correlations when performing nuclear calculations have been made (see, e.g., Refs. [1,2]). While collective phenomena have been known since the early times of nuclear physics, effects produced by short-range correlations (SRC) are more difficult to be experimentally singled out. The experimental and theoretical works in the past decade have provided us with a much clearer picture on the consequences of these correlations. There are clear signatures of the presence of correlation effects on some quantities related to the behavior of the single nucleon in nuclear medium. For instance, *NN* correlations are responsible for the reduction of the spectroscopic strengths of the nuclear hole states [1–3]. The theoretical understanding of this fact requires the knowledge of the removal spectral function which can be represented in a natural way by both overlap functions and single-nucleon spectroscopic factors [4]. They are directly related to observable quantities such as (p,d), $(e,e'p)$, and (γ,p) reaction cross sections. The comparison between the theoretically calculated and measured cross sections could serve as a test for the proper account of correlations within the theoretical approach considered.

Recently, a general procedure has been adopted [5] to extract the bound-state overlap functions and the associated spectroscopic factors and separation energies on the base of the ground-state one-body density matrix (OBDM). Initially, the procedure has been applied [6] to a model OBDM [7] accounting for SRC within the low-order approximation (LOA) to the Jastrow correlation method [8]. First, the applicability of the theoretically calculated overlap functions has been tested in the description of the ^{16}O(p,d) pickup reaction [9,10] and of the ^{40}Ca(p,d) reaction [9,11]. *The main result* from these investigations is that *absolute cross sections of the* (p,d) *reactions are evaluated without any additional normalization in contrast to standard distorted wave born approximation* (DWBA) *calculations*. Then, a detailed study of the cross sections of the electron- and photon-induced knockout reactions on ^{16}O [12] and ^{40}Ca [11] has been performed. The $(e,e'p)$ and (γ,p) reactions are more suitable to test various single-particle (SP) overlap functions and *NN* correlations. The theoretical results obtained in Refs. [11,12] reproduce with a fair agreement the shape of the experimental cross sections, in particular at large values of the missing momentum, where correlation effects are more sizable. Of course, the general success of the above procedure depends strongly on the availability of realistic one-body density matrices.

In the various approaches, the OBDM's are usually constructed for closed-shell nuclei. The ^{16}O nucleus has been studied by variational Monte Carlo [13] and Green function [14,15] methods. The treatment of heavier nuclei has not yet attained the same degree of accuracy as the light ones. The correlated basis function (CBF) theory, based on the Jastrow approach, has recently been extended to medium-heavy doubly closed-shell nuclei using Fermi hypernetted chain integral equations [16,17]. In addition, ^{16}O and ^{40}Ca nuclei have been examined by the generator coordinate method [18].

There is no systematic study of the one-body density matrix (and related quantities) which includes both closed- and open-shell nuclei. For that reason, in Ref. [19] expressions for the OBDM's $\rho(\mathbf{r},\mathbf{r}')$ and momentum distributions which could be used for both closed- and open-shell nuclei have been obtained. In Ref. [20] analytical expressions for the

charge form factors and densities of the s-p and s-d shell nuclei have been also derived. The $\rho(\mathbf{r},\mathbf{r}')$ was constructed using the factor cluster expansion of Clark and co-workers [21–23] and Jastrow correlation function which incorporates SRC for closed-shell nuclei. This approach was extrapolated to the case of $N=Z$ open-shell nuclei in Ref. [19]. Analyzing three different expansions it has been shown in Ref. [24] that they lead to almost equivalent results for important nuclear properties. The expressions for $\rho(\mathbf{r},\mathbf{r}')$ are functionals of the spherical harmonic oscillator (HO) orbitals and depend on the HO parameter and the correlation parameter. The values of the parameters which have been used for the closed-shell nuclei ^{4}He, ^{16}O, and ^{40}Ca were determined in Ref. [20] by a fit of the theoretical charge form factor, derived with the same cluster expansion, to the experimental one. For the open-shell nuclei ^{12}C, ^{24}Mg, ^{28}Si, and ^{32}S new values of these parameters have been obtained to give a better fit to the experimental data [19]. Moreover, these nuclei were treated as $1d$ shell nuclei and as $1d$-$2s$ shell nuclei. In the latter case, the A dependence of the high-momentum components of the momentum distributions becomes quite small.

The aim of the present work is to study the bound-state overlap functions for open-shell nuclei on the basis of Jastrow-type one-body density matrices for such nuclei. Next, the resulting overlap functions are tested in the description of nuclear observables, namely, the cross sections of (p,d) reactions on ^{24}Mg [25], ^{28}Si [26], and ^{32}S [25] and of the ^{32}S$(e,e'p)$ reaction [27]. Such an investigation allows us to examine the relationship between the OBDM and the associated overlap functions in that region of nuclei and also to estimate the role of SRC incorporated in the correlation approach used in the reaction cross section calculations.

The paper is organized as follows. A short description of the correlated OBDM of the target nucleus is given in Sec. II together with the procedure to extract the SP overlap functions from it. The results of the calculations are presented and discussed in Sec. III. The summary of the present work is given in Sec. IV.

II. THEORETICAL APPROACH

A. Correlated one-body density matrix

In order to evaluate the SP bound-state overlap functions, one needs the ground-state OBDM of the target nucleus which is defined by the expression

$$\rho(\mathbf{r},\mathbf{r}')=A\int \Psi^*(\mathbf{r},\mathbf{r}_2,\ldots,\mathbf{r}_A)\Psi(\mathbf{r}',\mathbf{r}_2,\ldots,\mathbf{r}_A) \times d\mathbf{r}_2\cdots d\mathbf{r}_A, \tag{1}$$

where $\Psi(\mathbf{r}_1,\mathbf{r}_2,\ldots,\mathbf{r}_A)$ is the normalized A-nucleon ground-state wave function. The integration in Eq. (1) is carried out over the radius vectors $\mathbf{r}_2$ to $\mathbf{r}_A$ and summation over spin variables is implied. In the present work, we start from a Jastrow-type trial many-particle wave function

$$\Psi(\mathbf{r}_1,\ldots,\mathbf{r}_A)=\mathcal{F}\Phi=\prod_{i<j}^{A} f(r_{ij})\Phi(\mathbf{r}_1,\ldots,\mathbf{r}_A), \tag{2}$$

where $\mathcal{F}$ is a model operator which introduces SRC, Φ is an uncorrelated (Slater determinant) wave function built up from single-particle wave functions which correspond to the occupied states, and $f(r_{ij})$ is the state-independent correlation function which was chosen to have the form

$$f(r_{ij})=1-\exp[-\beta(\mathbf{r}_i-\mathbf{r}_j)^2]. \tag{3}$$

The correlation function goes to 1 for large values of $r_{ij}=|\mathbf{r}_i-\mathbf{r}_j|$ and to 0 for $r_{ij}\to 0$. Apparently, the effect of SRC introduced by the function $f(r_{ij})$ becomes larger when the correlation parameter β becomes smaller and vice versa.

For our purpose, we represent the one-body density matrix $\rho(\mathbf{r},\mathbf{r}')$ by the form

$$\rho(\mathbf{r},\mathbf{r}')=\frac{\langle\Psi|\mathbf{O}_{\mathbf{rr}'}|\Psi'\rangle}{\langle\Psi|\Psi\rangle}=N\langle\Psi|\mathbf{O}_{\mathbf{rr}'}|\Psi'\rangle=N\langle\mathbf{O}_{\mathbf{rr}'}\rangle, \tag{4}$$

where $\Psi'=\Psi(\mathbf{r}_1',\mathbf{r}_2',\ldots,\mathbf{r}_A')$, N is the normalization factor and the integration is carried out over the vectors $\mathbf{r}_1$ to $\mathbf{r}_A$ and $\mathbf{r}_1'$ to $\mathbf{r}_A'$. The one-body "density operator" $\mathbf{O}_{\mathbf{rr}'}$ has the form

$$\mathbf{O}_{\mathbf{rr}'}=\sum_{i=1}^{A}\delta(\mathbf{r}_i-\mathbf{r})\,\delta(\mathbf{r}_i'-\mathbf{r}')\prod_{j\neq i}^{A}\delta(\mathbf{r}_j-\mathbf{r}_j'). \tag{5}$$

The same one-body operator has been used also in Ref. [28] [Eq. (14) of this reference] for realistic study of the nuclear transparency and the distorted momentum distributions in the semiinclusive process ^{4}He$(e,e'p)X$.

In order to evaluate the correlated one-body density matrix $\rho_{cor}(\mathbf{r},\mathbf{r}')$, we consider first the generalized integral

$$I(\alpha)=\langle\Psi|\exp[\alpha I(0)\mathbf{O}_{\mathbf{rr}'}]|\Psi'\rangle, \tag{6}$$

corresponding to the one-body "density operator" $\mathbf{O}_{\mathbf{rr}'}$ [given by Eq. (5)], from which we have

$$\langle\mathbf{O}_{\mathbf{rr}'}\rangle=\left[\frac{\partial\ln I(\alpha)}{\partial\alpha}\right]_{\alpha=0}. \tag{7}$$

For the cluster analysis of Eq. (7), after considering the subproduct integrals [21–23] and their factor cluster decomposition following the procedure of Ristig, Ter Low, and Clark, one can obtain an expression for the $\rho_{cor}(\mathbf{r},\mathbf{r}')$ [19],

$$\rho_{cor}(\mathbf{r},\mathbf{r}')\simeq N[\langle\mathbf{O}_{\mathbf{rr}'}\rangle_1-O_{22}(\mathbf{r},\mathbf{r}',\mathrm{g}_1)-O_{22}(\mathbf{r},\mathbf{r}',\mathrm{g}_2) +O_{22}(\mathbf{r},\mathbf{r}',\mathrm{g}_3)]. \tag{8}$$

The one-body contribution to the OBDM, $\langle\mathbf{O}'_{\mathbf{rr}}\rangle_1$ and the three terms $O_{22}(\mathbf{r},\mathbf{r}',\mathrm{g}_l)(l=1,2,3)$, which come from the two-body contribution, have the general forms

$$\langle\mathbf{O}'_{\mathbf{rr}}\rangle_1=\rho_{SD}(\mathbf{r},\mathbf{r}') =\frac{1}{\pi}\sum_{nl}\eta_{nl}(2l+1)\phi_{nl}^*(r)\phi_{nl}(r')P_l(\cos\omega'_{rr}), \tag{9}$$

and

$$O_{22}(\mathbf{r},\mathbf{r}',g_l)=4\sum_{n_il_i,n_jl_j}\eta_{n_il_i}\eta_{n_jl_j}(2l_i+1)(2l_j+1)\times\Bigg[4A^{n_il_in_jl_j,0}_{n_il_in_jl_j}(\mathbf{r},\mathbf{r}',g_l)-\sum_{k=0}^{l_i+l_j}\langle l_i0l_j0|k0\rangle^2A^{n_jl_jn_il_i,k}_{n_il_in_jl_j}(\mathbf{r},\mathbf{r}',g_l)\Bigg], \tag{10}$$

where η_{nl} are the occupation probabilities of the various states, $\phi_{nl}(r)$ are the radial SP wave functions, and

$$A^{n_3l_3n_4l_4,k}_{n_1l_1n_2l_2}(\mathbf{r},\mathbf{r}',g_1)=\frac{1}{4\pi}\phi^*_{n_1l_1}(r)\phi_{n_3l_3}(r')\times\exp[-\beta r^2]P_{l_3}(\cos\omega'_{rr})\times\int_0^\infty\phi^*_{n_2l_2}(r_2)\phi_{n_4l_4}(r_2)\times\exp[-\beta r_2^2]i_k(2\beta rr_2)r_2^2dr_2. \tag{11}$$

The matrix elements $A^{n_3l_3n_4l_4,k}_{n_1l_1n_2l_2}(\mathbf{r},\mathbf{r}',g_l)$ for $l=2$ and 3 have similar structure and are given in Ref. [19]. In the above expression $\omega_{rr'}$ is the angle between the vectors $\mathbf{r}$ and $\mathbf{r}'$ and $i_k(z)$ is the modified spherical Bessel function.

Expansion (8) of the present work has one- and two-body terms and the normalization of the wave function is preserved by the normalization factor N. The expressions of $\langle\mathbf{O}'_{\mathbf{rr}}\rangle_1$ and the three two-body terms $O_{22}(\mathbf{r},\mathbf{r}',g_l)(l=1,2,3)$ given by Eqs. (9) and (10) depend on the SP radial wave functions and so they are suitable to be used for analytical calculations with HO orbitals. These expressions were derived for the closed-shell nuclei with $N=Z$, where η_{nl} is 0 or 1. For the open-shell nuclei (with $N=Z$), we use the same expressions as in Refs. [19,20], where now $0\leqslant\eta_{nl}\leqslant1$. In this way, the systematic study of important quantities such as bound-state overlap functions and spectroscopic factors [9–12] can be extended to open-shell nuclei within the factor cluster expansion from Refs. [19,21–23].

It should be noted that a similar expression for $\rho_{cor}(\mathbf{r},\mathbf{r}')$ was derived by Gaudin *et al.* [29] in the framework of the LOA mentioned in the introduction. Their expansion contains one- and two-body terms and a part of the three-body terms so that the normalization property of the OBDM is fulfilled.

B. Overlap functions and their relation to the OBDM

The quantities related to the $(A-1)$-particle system, such as the overlap functions, the separation energies and the spectroscopic factors for its bound states can be fully determined in principle by the one-body density matrix for the ground state of the A-particle system [5]. This unique relationship holds generally for quantum many-body systems with sufficiently short-range forces between the particles and is based on the exact representation of the ground-state one-body density matrix [5]. The latter can be expressed in terms of the overlap functions $\phi_\alpha(\mathbf{r})$, which describe the residual nucleus as a hole state in the target, in the form

$$\rho(\mathbf{r},\mathbf{r}')=\sum_\alpha\phi^*_\alpha(\mathbf{r})\phi_\alpha(\mathbf{r}'). \tag{12}$$

In the case of a target nucleus with $J^\pi=0^+$ each of the bound-state overlap functions is characterized by the set of quantum numbers $\alpha\equiv nlj$, with n being the number of the state with a given multipolarity l and a total angular momentum j. The asymptotic behavior of the radial part of the neutron overlap functions for the bound states of the $(A-1)$ system is given by [5,30]

$$\phi_{nlj}(r)\rightarrow C_{nlj}\exp(-k_{nlj}r)/r, \tag{13}$$

where

$$k_{nlj}=\frac{1}{\hbar}[2m_{\mathrm{n}}(E^{A-1}_{nlj}-E^A_0)]^{1/2}. \tag{14}$$

In Eq. (14) m_{n} is the neutron mass, E^A_0 is the ground state energy of the target A nucleus, and E^{A-1}_{nlj} is the energy of the nlj state of the $(A-1)$ nucleus. For protons some mathematical complications arise due to an additional long-range part of the interaction originating from the Coulomb force, but the general conclusions of the consideration remain the same. The asymptotic behavior of the radial part of the corresponding proton overlap functions reads

$$\phi_{nlj}(r)\rightarrow C_{nlj}\exp[-k_{nlj}r-\eta\ln(2k_{nlj}r)]/r, \tag{15}$$

where η is the Coulomb (or Sommerfeld) parameter and k_{nlj} (14) contains the mass of the proton.

The lowest $n=n_0$ neutron lj-bound-state overlap function is determined by the asymptotic behavior of the associated partial radial contribution of the one-body density matrix $\rho_{lj}(r,r')(r'=a\rightarrow\infty)$ and Eqs. (12) and (13) lead to the expression

$$\phi_{n_0lj}(r)=\frac{\rho_{lj}(r,a)}{C_{n_0lj}\exp(-k_{n_0lj}a)/a}, \tag{16}$$

where the constants C_{n_0lj} and k_{n_0lj} are completely determined by $\rho_{lj}(a,a)$. In this way the separation energy

$$\epsilon_{n_0lj}\equiv E^{A-1}_{n_0lj}-E^A_0=\frac{\hbar^2k^2_{n_0lj}}{2m_{\mathrm{n}}} \tag{17}$$

and the spectroscopic factor $S_{n_0lj}=\langle\phi_{n_0lj}|\phi_{n_0lj}\rangle$ can be determined as well.

The applicability of this theoretical scheme has been demonstrated in Refs. [6,9–12] by means of realistic one-body density matrices of ^{16}O and ^{40}Ca constructed within different correlation methods. In particular, the calculated overlap

functions corresponding to the OBDM's from various approaches to the CBF theory [17,31] have shown the substantial deviation of their shapes with respect to the Hartree-Fock (HF) wave functions [10]. The inclusion of short-range and tensor correlations has caused a depletion of the levels below Fermi level which is reflected in the substantial reduction of the spectroscopic factors for the quasihole states.

Thus, having the procedure for calculating such important quantities as the overlap functions and the spectroscopic factors one can apply it to the one-body density matrices of some open *s*-*d* shell nuclei. In order to reveal better the nuclear structure properties in this region of nuclei and to draw a parallel with the closed-shell ones, it is desirable to test the resulting overlap functions in calculations of one-nucleon pickup and knockout reactions, which is the aim of the present paper.

In the end of this section, we would like to note that the starting point for the present calculations are OBDM's which include SRC of central Jastrow type, and which have been computed by a cluster expansion to leading order in the correlation function. Similar approach has been very recently used to study the effects of SRC on the $(e,e'p)$ exclusive response functions and cross sections [32]. In both calculations, the radial dependence of the correlated function [Eq. (3)] is restricted to Gaussian like one. As well known [10,31,33,34], the inclusion of state-dependent correlations, in particular of tensor ones, is important when modeling transfer reactions. In addition, long-range correlations should also be taken into account in a consistent way. On the other hand, we use in our calculations HO single-particle wave functions, which do not have the correct exponential behavior in the asymptotic region, to construct the OBDM. It has been already pointed out in previous works [11,32] that an important condition of the numerical procedure is the exponential asymptotics of the overlap functions at $r' \to \infty$ [see Eqs. (13) and (15)], which is related to the correct asymptotics of $\rho_{lj}(r,r')$ at $r' \to \infty$. This imposed the development of a method, though not unique, in Ref. [6] to overcome the difficulties arising from the HO single-particle wave function asymptotics. The condition for the correct asymptotics is fulfilled in Refs. [11,32] by using of a SP basis obtained with a Woods-Saxon potential. The use of HO wave functions in the present work instead of more realistic Woods-Saxon ones following the method from Ref. [6] allows us, however, to obtain analytical expressions for the OBDM's. At present, no model correlated one-body density matrices treating open *s*-*d* shell nuclei are available except that of Ref. [19] and, therefore, this work should be considered as an initial attempt to study the relative importance of the effects of both SRC and particular structure of these nuclei on overlap functions, spectroscopic factors, and reaction cross sections.

III. RESULTS OF CALCULATIONS AND DISCUSSION

The one-body density matrices (8) constructed by using of factor cluster expansion have been applied to calculate neutron and proton overlap functions including NN correlations and related to possible $1p$-, $1d$-, and $2s$-quasihole states in the ^{24}Mg, ^{28}Si, and ^{32}S nuclei. We note that in our work the extracted overlap functions are not separated with respect to the spin-orbit partners $j = l \pm 1/2$. Although the OBDM's do not allow to obtain different results for $d_{3/2}$ and $d_{5/2}$ quasihole states, it is useful in some calculations of reaction cross sections for transitions to these states to test the overlap function corresponding to the $1d$ bound state.

TABLE I. Neutron and proton spectroscopic factors (SF) and separation energies (ϵ_n and ϵ_p in MeV) calculated on the basis of the one-body density matrices [19] for ^{24}Mg, ^{28}Si, ^{32}S, and ^{40}Ca. Comparison is made with the experimental data ϵ_n^{exp} and ϵ_p^{exp} for the separation energies [25–27,41,42].

		Neutrons			Protons		
Nucleus	nl	ϵ_n	ϵ_n^{exp}	SF	ϵ_p	ϵ_p^{exp}	SF
^{24}Mg	$1p$	18.85	19.29	0.9474	14.13	14.33	0.9798
	$1d$	16.94	16.53	0.4026	11.02	11.69	0.4586
	$2s$	18.37	18.89	0.4706	13.63	14.08	0.5414
^{28}Si	$1p$	21.34	21.35	0.8528	15.21	15.64	0.9788
	$1d$	17.29	17.18	0.5071	11.49	11.59	0.6265
	$2s$	17.32	17.96	0.3958	12.09	12.43	0.4675
^{32}S	$1p$	22.54	22.80	0.7454	15.68	16.29	0.8856
	$1d$	16.98	17.33	0.5682	9.82	10.13	0.6636
	$2s$	14.75	15.09	0.4712	8.53	8.86	0.5648
^{40}Ca	$1d$	15.45	15.64	0.7691	8.34	8.33	0.6729
	$2s$	17.86	18.19	0.8001	10.33	10.94	0.8051

The values of the spectroscopic factors (SF) and of the separation energies for neutrons and protons deduced from the calculations are listed in Table I. The separation energies (17) derived from the procedure are in acceptable agreement with the corresponding empirical ones. As a common feature, a substantial reduction of the spectroscopic factors of the states which are below the Fermi level (of the independent-particle picture) is observed for all nuclei considered due to the short-range NN correlations and their particular open-shell structure. For instance, the values of the SF for the states with $l=0$ and $l=2$ are much smaller than the values obtained for the $l=1$ state. The particular features of the nuclear structure in the $2s$-$1d$ region (in which the $1p$ state is not a valence one) are responsible for the larger reduction of the spectroscopic factors of the levels, though partly occupied, in these open *s*-*d* shell nuclei in comparison with the ''more occupied'' $1p$ quasihole state. It can be also seen from Table I that the trend of the calculated SF for proton bound states follows that one corresponding to the neutron overlap functions.

We would like to note the larger reduction of the spectroscopic factors corresponding to quasihole states of the open-shell nuclei considered in comparison with the spectroscopic factors for the states in closed-shell ^{16}O [6,10] and ^{40}Ca [6] nuclei when SRC are taken into account. To discuss this point, first we give in Table I the spectroscopic factors for the $1d$ and $2s$ quasihole states of the closed-shell ^{40}Ca deduced from the one-body density matrix calculations within the same Jastrow approach [19] used in the present work. For comparison, the SRC accounted for within the LOA to the Jastrow correlation method [6] produce spectroscopic factors

of 0.892 for the $1d$ state and 0.956 for the $2s$ in ^{40}Ca nucleus. It turns out that the method from Ref. [19] leads to a suppression of the spectroscopic factors for the closed-shell ^{40}Ca nucleus. The reason for the different SF values could be related to the details of the calculations with the Jastrow approach, when using the two cluster expansions. Particularly, they concern the truncation of the expansions mentioned already in Sec. II, which causes a different account for the SRC (although they are of the same Jatrow type), as well as the different asymptotic behavior of the OBDM obtained in both expansions. In our opinion, the mentioned features of the method from Ref. [19] lead to an additional reduction of the values of the SF for open-shell nuclei as well. To support this, we would like to note the comparison of both cluster expansions given in Ref. [24] on the example of the nucleon momentum distributions $n(k)$ of various nuclei. The high-momentum tails of $n(k)$ obtained using LOA [7] underestimate the corresponding ones obtained with the use of the cluster expansion of Clark and co-workers [19] for the nuclei considered. In this way, the smaller values for the spectroscopic factors derived in the present work within Ref. [19] for both closed- and open-shell nuclei reflect the stronger accounting for the SRC and can be understood. As a common feature, the spectroscopic factors for the s-d open-shell nuclei are smaller than those for the closed-shell nuclei.

Second, in order to check our theoretically calculated spectroscopic factors it is useful to compare them with some single-particle occupation probabilities available for the considered $1d$-$2s$ shell nuclei. The HF calculations performed in Ref. [35] for the (p,p') scattering analyses treating protons and neutrons equivalently yield values of 0.479 and 0.682, respectively, for the $1d_{5/2}$ fractional occupancies of ^{24}Mg and ^{28}Si. The $2s_{1/2}$ proton occupancy of 0.67(9) derived for ^{32}S was reported in Ref. [36]. As can be seen from Table I our calculated spectroscopic factors for these states are smaller than the resulting occupancies, thus, satisfying the general property $S_{nlj} \leqslant N_{nlj}^{max}$, i.e., in each lj subspace the spectroscopic factor S_{nlj} is smaller than the largest natural occupation number N_{nlj}^{max} [5].

Generally, the values of the spectroscopic factors for open-shell nuclei are influenced by the presence of SRC accounted for in our OBDM similar to the case of the closed-shell nuclei. However, in our approach an additional reduction of the spectroscopic factors for open $1d$-$2s$ shell nuclei takes place because the SF contain themselves a structure information for the noncomplete shell occupancy in these nuclei. This conclusion is confirmed by the check of the normalization condition for the OBDM [Eq. (12)].

The DWBA calculations of the pickup reactions on the considered open-shell nuclei were performed using the DWUCK4 code [37] assuming zero-range approximation for the p-n interaction inside the deuteron. The same approach has been adopted in previous analyses of (p,d) reactions on ^{16}O [9,10] and ^{40}Ca [9,11]. The values of the optical potential parameters have been taken in each case to be the same as in the corresponding standard DWBA calculations.

The standard DWUCK4 procedure is performed by calculating the bound-neutron wave function using the separation energy prescription (SEP) and different sets of proton and deuteron optical model parameters. The optical potential is defined to be

$$V_{opt} = -Vf(x_0) - i\left(W - 4W_D \frac{d}{dx_D}\right) f(x_D) - \left(\frac{\hbar}{m_\pi c}\right)^2 V_{s.o.}(\mathbf{L}\cdot\boldsymbol{\sigma}) \frac{1}{r}\frac{d}{dr} f(x_{s.o.}) + V_c, \quad (18)$$

where

$$f(x_i) = [1+\exp(x_i)]^{-1}, \quad x_i = (r - r_i A^{1/3})/a_i, \quad (19)$$

and V_c is the Coulomb potential of a uniformly charged sphere of radius $r_c A^{1/3}$. The proton and deuteron optical model parameters we use are those of Källne and Fagerström [25] for ^{24}Mg and ^{32}S and those of Sundberg and Källne [26] for ^{28}Si at $E_p = 185$ MeV incident energy.

The results for the differential cross sections for the ^{24}Mg(p,d), ^{28}Si(p,d), and ^{32}S(p,d) reactions at incident proton energy $E_p = 185$ MeV compared with the experimental data are presented in Figs. 1, 2, and 3, respectively. In each panel, the results obtained with overlap function, with bound-state wave function following the standard DWBA procedure within the SEP and with uncorrelated shell-model wave function are plotted. As can be seen, in general, the use of overlap functions derived from the one-body density matrix calculations leads to a qualitative agreement with the experimental data reproducing the amplitude of the first maximum and qualitatively the shape of the differential cross section. In this case no extra spectroscopic factor is needed, since our overlap functions already include the associated spectroscopic factors. In the examples of some reactions the standard DWBA form factor is also able to reproduce the shape of cross sections, while the uncorrelated wave functions fail to describe correctly neither the size nor the shape of the angular distributions. The differences between the three types of calculations are observed mostly at larger angles where the curves corresponding to the uncorrelated case overestimate substantially the experimental data. Thus, the relevant importance of SRC included in our approach becomes clear for a correct description of pickup processes and this makes it possible to conclude that the replacement of the overlap integral by a single-particle wave function is a rough approximation.

We would like to note that our results for the (p,d) cross sections with the use of overlap functions are obtained without any additional normalization, while the standard DWBA curves and those corresponding to the uncorrelated case need an adjustment by a fitting parameter, i.e., the phenomenological spectroscopic factor. The values of these spectroscopic factors are given in Table II and can be compared with our theoretically calculated spectroscopic factors from Table I. For instance, the values of the phenomenological spectroscopic factors deduced from the traditional DWBA calculations for the transitions to $5/2^+$ and $3/2^+$ in ^{23}Mg are very close to the empirical values obtained in Ref. [25], although a clear physical interpretation could not be done.

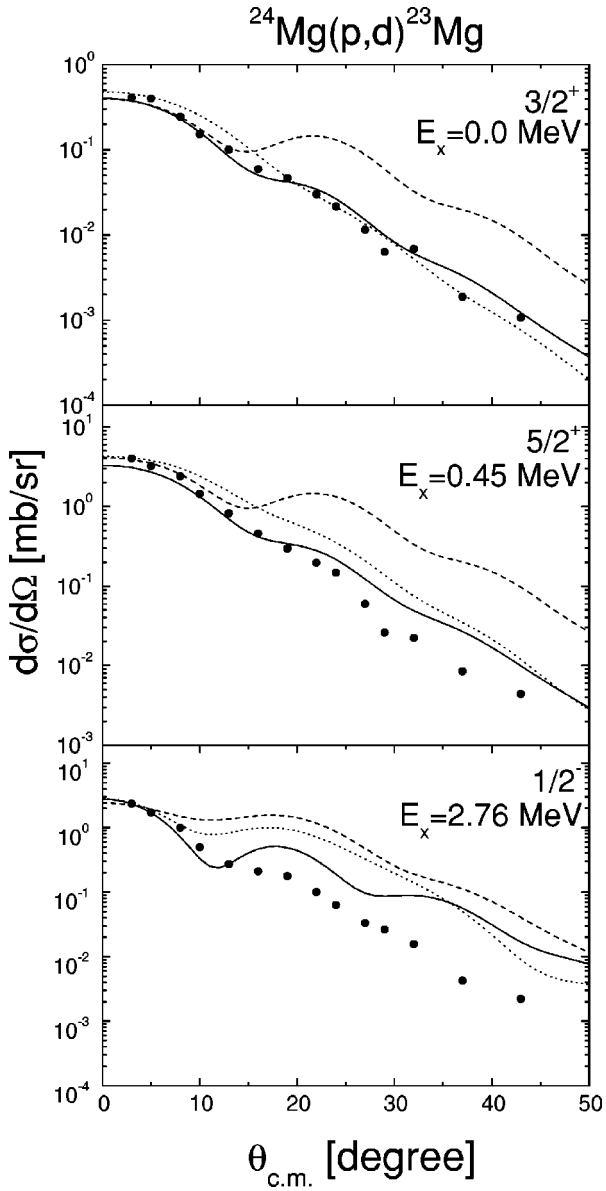

FIG. 1. Differential cross section for the ^{24}Mg(p,d) reaction at incident proton energy $E_p=185$ MeV to the $3/2^+$ ground and to the $5/2^+$ and $1/2^-$ excited states in ^{23}Mg. The neutron overlap functions are derived from the OBDM (solid line). The calculated standard DWBA curve (dotted line) and the uncorrelated SM result (dashed line) are also presented. The experimental data [25] are given by the full circles.

Figure 1 shows the differential cross sections for the transitions to the ground $3/2^+$ state and to the excited $5/2^+$ (at excitation energy $E_x=0.45$ MeV) and $1/2^-$ (at $E_x=2.76$ MeV) states in ^{23}Mg nucleus. A comparison with the experimental data from Ref. [25] is also made. As can be seen our calculations using the overlap function for the transition to the ground $3/2^+$ state agree fairly well with the experimental angular distribution for the same transition reproducing the amplitude of the first maximum and qualitatively the shape of the differential cross section. *We emphasize that this result is obtained without any additional normalization since the calculated overlap function for 3/2$^+$ state already includes the spectroscopic factor of 0.4* (see Table I). Moreover, at larger angles our calculations lead to better agreement with the experimental data comparing with the standard DWBA analysis. In the latter, the overlap function is replaced by a SP wave function corresponding to a given mean-field potential. In such calculations the *NN* correlations are included approximately by adjusting the mean-field potential parameter values. Another reason for the observed discrepancies in Ref. [25] is that a spherical potential has been used for generating the bound-neutron state in DWBA instead of a more realistic deformed one. We would like to mention here *the principal role of the overlap function for the good description of the differential cross section* for the transition to the ground $3/2^+$ state in ^{23}Mg. It is obtained on the basis of a correlated OBDM and allows one to account for the short-range correlations in the case of pickup reaction. The results of the calculations carried out additionally for the transitions to the excited states are less satisfactory for angles larger than ten degrees. One of the reasons for this is the unrealistic (HO) asymptotic behavior of the Jastrow-type OBDM [19] which has been used to calculate the overlap functions following the method described in Sec. II. Concerning the similarity of the shape of the theoretical curves (though different by one order of magnitude) in the upper and middle panels of Fig. 1, we note that for the ground state the $1d_{3/2}$ overlap function is needed while for the first excited state the $1d_{5/2}$ overlap function is needed. The usage of a common $1d$ overlap function in our work obviously gives a larger deviation from the data for the latter case. On the other hand, a large fragmentation of the single-particle strengths is a common feature of the studied $2s$-$1d$ nuclei. For example, pickup from the $1p_{1/2}$ and $1p_{3/2}$ subshells in $2s$-$1d$ nuclei has been an intriguing topic from experimental point of view [25] indicating several $1p$ states observed in ^{23}Mg.

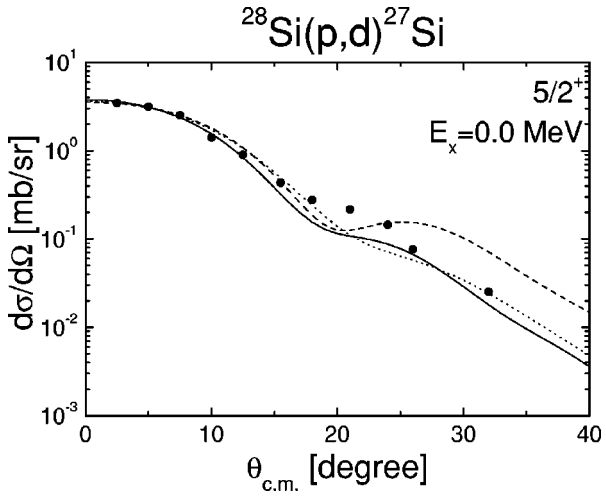

FIG. 2. Differential cross section for the ^{28}Si(p,d) reaction at incident proton energy $E_p=185$ MeV to the $5/2^+$ ground state in ^{27}Si. The neutron overlap functions are derived from the OBDM (solid line). The calculated standard DWBA curve (dotted line) and the uncorrelated SM result (dashed line) are also presented. The experimental data [26] are given by the full circles.

Figure 2 shows the ground-state differential cross section

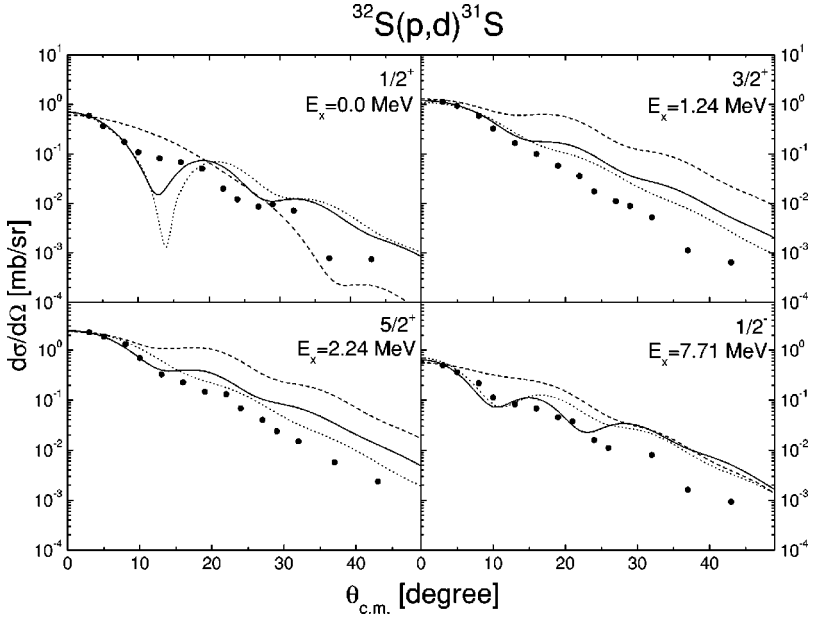

FIG. 3. Differential cross section for the ^{32}S(p,d) reaction at incident proton energy $E_p = 185$ MeV to the $1/2^+$ ground and to the $3/2^+$, $5/2^+$, and $1/2^-$ excited states in ^{31}S. The neutron overlap functions are derived from the OBDM (solid line). The calculated standard DWBA curve (dotted line) and the uncorrelated SM result (dashed line) are also presented. The experimental data [25] are given by the full circles.

of the reaction ^{28}Si$(p,d)^{27}$Si with $1d_{5/2}$ neutron pickup, while the angular distributions of the reaction ^{32}S$(p,d)^{31}$S for the transition to the ground $1/2^+$ state and to the excited $3/2^+$ (at $E_x = 1.24$ MeV), $5/2^+$ (at $E_x = 2.24$ MeV), and $1/2^-$ (at $E_x = 7.71$ MeV) states in ^{31}S nucleus are shown in Fig. 3. In general, a quantitative agreement of the calculations with the experimental cross sections in the region of the first maximum is obtained for all states of the residual ^{27}Si and ^{31}S nuclei. The presence of admixtures of various states observed in the ground state of ^{32}S [25] is responsible for a poorer description of these (p,d) data. The behavior of the theoretically calculated angular distribution and the comparison with the data for the transition to the strongly excited $1/2^-$ are similar to those for $l=1$ transfer in ^{24}Mg$(p,d)^{23}$Mg.

In order to see the sensitivity of the results to the optical potential parameters, we examine the transition to the ground $5/2^+$ state in ^{27}Si nucleus. In Fig. 4 three different theoretical curves are given with respect to deuteron optical potential parameter values used in the calculations. Particularly, the effects of changing the radius of the real part of this potential R_d is shown. The best agreement with the experimental data is achieved with the value of $R_d = 0.80$ fm giving also the best DWBA fit in Ref. [26]. It can be noted that the choice of the radius of the real part of the deuteron optical potential within the interval from 0.65 fm to 0.95 fm (considered in the standard DWBA analyses) does not influence strongly the good overall agreement of the cross sections obtained by means of the theoretically calculated overlap function with the experimental data. Apart from the shown sensitivity of the calculations to the deuteron optical potential, in general, we should mention that the (p,d) reaction is more sensitive to the reaction mechanism adopted than to the choice of the bound-state wave function. Nevertheless, it is seen from Fig. 4 that our theoretically calculated overlap function corre-

TABLE II. Phenomenological spectroscopic factors S_{DWBA} deduced from the standard DWBA calculations and S_{SM} deduced from the calculations with uncorrelated shell-model (SM) OBDM's of Ref. [19] for the reactions considered in Figs. 1–3.

Reaction	nl_j	S_{DWBA}	S_{SM}
^{24}Mg$(p,d)^{23}$Mg	$1d_{3/2}$	0.25	0.10
	$1d_{5/2}$	2.50	1.00
	$1p_{1/2}$	1.11	0.75
^{28}Si$(p,d)^{27}$Si	$1d_{5/2}$	2.13	2.13
^{32}S$(p,d)^{31}$S	$2s_{1/2}$	0.33	0.56
	$1d_{3/2}$	1.43	1.00
	$1d_{5/2}$	4.00	1.00
	$1p_{1/2}$	1.00	0.11

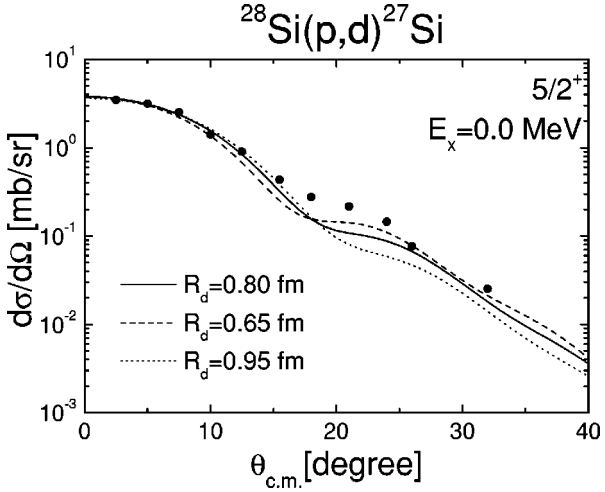

FIG. 4. Differential cross section for the ^{28}Si(p,d) reaction at incident proton energy $E_p = 185$ MeV to the $5/2^+$ ground state in ^{27}Si. Line convention referring to calculations using different optical potential parameter values and neutron overlap function derived from the OBDM is given (see also the text). The experimental data [26] are given by the full circles.

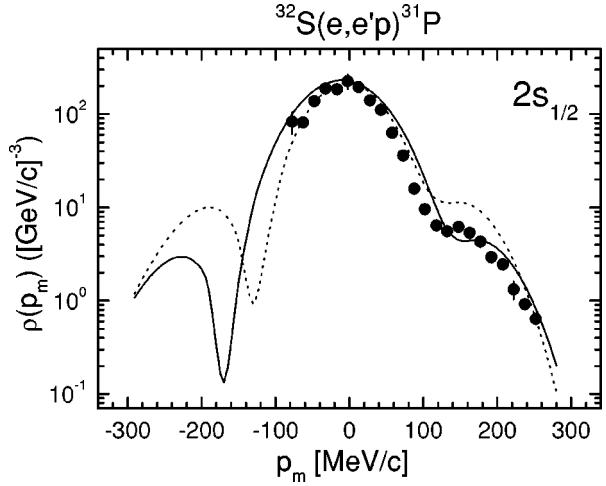

FIG. 5. Reduced cross section of the $^{32}S(e,e'p)$ reaction as a function of the missing momentum p_m for the transition to the $1/2^+$ ground state of ^{31}P. The proton overlap function is derived from the OBDM (solid line). The result with the uncorrelated (HO) wave function is given by dotted line. The experimental data (full circles) are taken from Ref. [27].

sponding to the $1d$ bound state is able to reproduce well the absolute cross section.

We have analyzed the (p,d) pickup reaction in ^{24}Mg, ^{28}Si, and ^{32}S at proton incident energy of 185 MeV. Unfortunately, little is known about the deuteron optical potentials at high energies and the discrepancies with the experimental data might be partly attributed to the uncertainties in the determination of the optical potentials. This also makes difficult to separate clearly the role of the overlap functions associated with the single-neutron bound states. We emphasize, however, the important general necessity the overlap functions to be calculated on the basis of realistic OBDM's and only then the sensitivity to all other ingredients of the theoretical schemes to be analyzed.

It turned out from the previous analyzes of one-nucleon removal reactions [11,12] that the quasifree nucleon knockout is more suitable to investigate the role of overlap functions as bound-state wave functions. An example of electron-induced proton knockout from ^{32}S for the transition to the ground $2s_{1/2}$ state of ^{31}P is given in Fig. 5. Calculations have been done with the code DWEEPY [38], which is based on the nonrelativistic distorted wave impulse approximation (DWIA) description of the nucleon knockout process and includes final-state interactions and Coulomb distortion of the electron waves [39]. The latter has been treated with a high-energy expansion in inverse powers of the electron energy [38]. In the figure, the result obtained with the proton overlap function for the $2s$ state of ^{32}S and the optical potential from Ref. [40] is compared with the NIKHEF data from Ref. [27]. A reasonable agreement with the experimental data for the reduced cross section is obtained. In the analysis of Ref. [27] the calculations are performed within the same DWIA framework and with the same optical potential, but a phenomenological single-particle wave function is used with a radius adjusted to the data. *We emphasize that in the present work the overlap function is theoretically calculated on the basis of the Jastrow-type OBDM of ^{32}S and does not contain any free parameters*. It can be seen from Fig. 5 that our spectroscopic factor of 0.5648 gives a good agreement with the size of the experimental cross section and, in addition, it is in accordance with the integrated strength for the valence $2s_{1/2}$ shell in ^{32}S [27] which amounts to 65(7)% of the SP strength obtained using the shell-model bound-state function. The result for the $^{32}S(e,e'p)$ cross section obtained with the harmonic-oscillator bound-state wave function is also illustrated in Fig. 5. It has been computed with the same oscillator parameter value $b=2$ fm for the $2s_{1/2}$ ground-state wave function as in the original calculations of the OBDM without SRC [19]. In order to perform a consistent comparison with the result when considering theoretically calculated overlap function, we have applied the same spectroscopic factor of 0.5648. In this case, the size of the reduced cross section is also reproduced, but the HO wave function gives much worse description of the experimental data [27]. Thus, the comparison made in Fig. 5 shows the important role of the SRC accounted for in our approach for the correct description of knockout reactions.

We have also performed calculations for the transition to the excited $1d_{5/2}$ state at $E_x=2.234$ MeV and have found in good agreement with the shape of the experimental momentum distribution. In our opinion, however, the comparison for the $1d$ states is not very meaningful since our approach cannot discriminate between the $d_{5/2}$ and $d_{3/2}$ states and the proton overlap function is calculated for the $1d$ state. From the experimental point of view, it is noted in Ref. [27] that it is also impossible to distinguish strengths originating from both $1d$ shells for the integrated $l=2$ strength. In this sense, our spectroscopic factor of 0.6636 fits the integrated spectroscopic strength well in the $1d$ shell up to 24 MeV excitation energy (the value 6.04(60) from Table V in Ref. [27]), thus, representing a depletion of about 60% of the full $1d$ shell.

IV. CONCLUSIONS

The results of the present work can be summarized as follows:

(i) Single-particle overlap functions, spectroscopic factors, and separation energies are calculated from the Jastrow-type one-body density matrices, which were derived using factor cluster expansion, for the ground state of the open-shell ^{24}Mg, ^{28}Si, and ^{32}S nuclei.

(ii) Taking into account both short-range correlations and specific nuclear structure it is found that the deduced spectroscopic factors S_{nlj} of the hole states of open-shell nuclei in our particular Jastrow approach are substantially smaller than those of the closed-shell ones satisfying at the same time the general relation with the natural occupation probabilities N_{nlj}, namely, $S_{nlj} \leqslant N_{nlj}^{max}$.

(iii) The absolute values of the differential cross sections of (p,d) reactions on ^{24}Mg, ^{28}Si, and ^{32}S as well as of $^{32}S(e,e'p)$ reduced cross section are calculated by using the theoretically obtained overlap functions which already contain *NN* correlations. The acceptable agreement with the

experimental data shows that this method is applicable also to the case of open-shell nuclei. The description of the cross sections might be improved including the deformation effects in the even-even $Z=N$ nuclei in the $2s$-$1d$ region.

(iv) Using more realistic OBDM's with a correct asymptotic behavior one can expect that the resulting overlap functions will be able to describe more accurately the experimental cross sections of the one-nucleon removal reactions on open s-d shell nuclei. In this case more definite conclusions about the role of the SRC in open- and closed-shell nuclei can be drawn.

ACKNOWLEDGMENTS

The authors are grateful to Dr. L. Lapikás for providing us the experimental data from Ref. [27] and for the fruitful discussions with him and Professor K. Amos. This work was partly supported by the Bulgarian National Science Foundation under Contract Nos. Φ−809 and Φ−905.

[1] A.N. Antonov, P.E. Hodgson, and I. Zh. Petkov, *Nucleon Momentum and Density Distributions in Nuclei* (Clarendon, Oxford, 1988).
[2] A.N. Antonov, P.E. Hodgson, and I. Zh. Petkov, *Nucleon Correlations in Nuclei* (Springer-Verlag, Berlin, 1993).
[3] L. Lapikás, Nucl. Phys. **A553**, 297c (1993).
[4] A.N. Antonov, M.V. Stoitsov, M.K. Gaidarov, S.S. Dimitrova, and P.E. Hodgson, J. Phys. G **21**, 1333 (1995).
[5] D. Van Neck, M. Waroquier, and K. Heyde, Phys. Lett. B **314**, 255 (1993).
[6] M.V. Stoitsov, S.S. Dimitrova, and A.N. Antonov, Phys. Rev. C **53**, 1254 (1996).
[7] M.V. Stoitsov, A.N. Antonov, and S.S. Dimitrova, Phys. Rev. C **47**, R455 (1993); **48**, 74 (1993); Z. Phys. A **345**, 359 (1993).
[8] R. Jastrow, Phys. Rev. **98**, 1479 (1955).
[9] S.S. Dimitrova, M.K. Gaidarov, A.N. Antonov, M.V. Stoitsov, P.E. Hodgson, V.K. Lukyanov, E.V. Zemlyanaya, and G.Z. Krumova, J. Phys. G **23**, 1685 (1997).
[10] M.K. Gaidarov, K.A. Pavlova, S.S. Dimitrova, M.V. Stoitsov, A.N. Antonov, D. Van Neck, and H. Müther, Phys. Rev. C **60**, 024312 (1999).
[11] M.V. Ivanov, M.K. Gaidarov, A.N. Antonov, and C. Giusti, Phys. Rev. C **64**, 014605 (2001).
[12] M.K. Gaidarov, K.A. Pavlova, A.N. Antonov, M.V. Stoitsov, S.S. Dimitrova, M.V. Ivanov, and C. Giusti, Phys. Rev. C **61**, 014306 (2000).
[13] S.C. Pieper, R.B. Wiringa, and V.R. Pandharipande, Phys. Rev. C **46**, 1741 (1992).
[14] W.H. Dickhoff and H. Müther, Rep. Prog. Phys. **55**, 1947 (1992).
[15] A. Polls, H. Müther, and W.H. Dickhoff, in *Proceedings of the Conference on Perspectives in Nuclear Physics at Intermediate Energies*, Trieste, 1995, edited by S. Boffi, C. Ciofi degli Atti, and M.M. Giannini (World Scientific, Singapore, 1996), p. 308.
[16] G. Co', A. Fabrocini, S. Fantoni, and I.E. Lagaris, Nucl. Phys. **A549**, 439 (1992).
[17] F. Arias de Saavedra, G. Co', A. Fabrocini, and S. Fantoni, Nucl. Phys. **A605**, 359 (1996).
[18] M.V. Ivanov, A.N. Antonov, and M.K. Gaidarov, Int. J. Mod. Phys. E **9**, 339 (2000).
[19] Ch.C. Moustakidis and S.E. Massen, Phys. Rev. C **62**, 034318 (2000).
[20] S.E. Massen and Ch.C. Moustakidis, Phys. Rev. C **60**, 024005 (1999).
[21] J.W. Clark and M.L. Ristig, Nuovo Cimento A **70**, 313 (1970).
[22] M.L. Ristig, W.J. Ter Low, and J.W. Clark, Phys. Rev. C **3**, 1504 (1971).
[23] J.W. Clark, Prog. Part. Nucl. Phys. **2**, 89 (1979).
[24] Ch.C. Moustakidis, S.E. Massen, C.P. Panos, M.E. Grypeos, and A.N. Antonov, Phys. Rev. C **64**, 014314 (2001).
[25] J. Källne and B. Fagerström, Phys. Scr. **11**, 79 (1975).
[26] O. Sundberg and J. Källne, Ark. Fys. **39**, 323 (1969).
[27] J. Wesseling, C.W. de Jager, L. Lapikás, H. de Vries, M.N. Harakeh, N. Kalantar-Nayestanaki, L.W. Fagg, R.A. Lindgren, and D. Van Neck, Nucl. Phys. **A547**, 519 (1992).
[28] H. Morita, C. Ciofi degli Atti, and D. Treleani, Phys. Rev. C **60**, 034603 (1999).
[29] M. Gaudin, J. Gillespie, and G. Ripka, Nucl. Phys. **A176**, 237 (1971).
[30] J.M. Bang, F.A. Gareev, W.T. Pinkston, and J.S. Vaagen, Phys. Rep. **125**, 253 (1985).
[31] D. Van Neck, L. Van Daele, Y. Dewulf, and M. Waroquier, Phys. Rev. C **56**, 1398 (1997).
[32] M. Mazziotta, J.E. Amaro, and F. Arias de Saavedra, Phys. Rev. C **65**, 034602 (2002).
[33] A. Fabrocini and G. Co', Phys. Rev. C **63**, 044319 (2001).
[34] J. Ryckebusch, Phys. Rev. C **64**, 044606 (2001).
[35] K. Amos, J. Morton, I. Morrison, and R. Smith, Aust. J. Phys. **31**, 1 (1978).
[36] J. Wesseling, C.W. de Jager, L. Lapikás, H. de Vries, L.W. Fagg, M.N. Harakeh, N. Kalantar-Nayestanaki, R.A. Lindgren, E. Moya De Guerra, and P. Sarriguren, Phys. Rev. C **55**, 2773 (1997).
[37] K. Langanke, J.A. Maruhn, and S.E. Koonin, *Computational Nuclear Physics 2: Nuclear Reactions* (Springer-Verlag, Berlin, 1993), p. 88.
[38] C. Giusti and F.D. Pacati, Nucl. Phys. **A473**, 717 (1987); **A485**, 461 (1988).
[39] S. Boffi, C. Giusti, F.D. Pacati, and M. Radici, *Electromagnetic Response of Atomic Nuclei, Oxford Studies in Nuclear Physics* (Clarendon, Oxford, 1996).
[40] P. Schwandt, H.O. Meyer, W.W. Jacobs, A.D. Bacher, S.E. Vigdor, M.D. Kaitchuck, and T.R. Donoghue, Phys. Rev. C **26**, 55 (1982).
[41] P.M. Endt and C. van der Leun, Nucl. Phys. **A105**, 1 (1967).
[42] C. Mahaux and R. Sartor, Nucl. Phys. **A528**, 253 (1991).